Author Manuscript

Author Manuscript

Author Manuscript

Author Manuscript

HHS Public Access

Author manuscript

Anal Chem. Author manuscript; available in PMC 2024 January 31.

Published in final edited form as:

Anal Chem. 2023 July 11; 95(27): 10204–10210. doi:10.1021/acs.analchem.3c00374.

Hydrogen–Deuterium Exchange Epitope Mapping of Glycosylated Epitopes Enabled by Online Immobilized Glycosidase

Timothy R. O'Leary,
Department of Molecular Medicine, The Herbert Wertheim UF Scripps Institute for Biomedical Innovation & Technology, Jupiter, Florida 33458, United States

Deepa Balasubramaniam,
Lilly Biotechnology Center, Eli Lilly and Company, San Diego, California 92121, United States

Kristin Hughes,
Lilly Biotechnology Center, Eli Lilly and Company, San Diego, California 92121, United States

Denisa Foster,
Lilly Biotechnology Center, Eli Lilly and Company, San Diego, California 92121, United States

Jeffrey Boyles,
Eli Lilly and Company, Indianapolis, Indiana 46225, United States

Kristina Coleman,
Lilly Biotechnology Center, Eli Lilly and Company, San Diego, California 92121, United States

Patrick R. Griffin
Department of Molecular Medicine, The Herbert Wertheim UF Scripps Institute for Biomedical Innovation & Technology, Jupiter, Florida 33458, United States

Abstract

Hydrogen–deuterium exchange coupled with mass spectrometry (HDX–MS) is widely used for monoclonal antibody (mAb) epitope mapping, which aids in the development of therapeutic mAbs and vaccines, as well as enables the understanding of viral immune evasion. Numerous mAbs are known to recognize N-glycosylated epitopes and to bind in close proximity to an *N*-glycan site; however, glycosylated protein sites are typically obscured from HDX detection as a result of the inherent heterogeneity of glycans. To overcome this limitation, we covalently immobilized the glycosidase PNGase Dj on a solid resin and incorporated it into an online HDX–MS workflow for post-HDX deglycosylation. The resin-immobilized PNGase Dj exhibited robust tolerance to

Corresponding Author: Patrick R. Griffin – Department of Molecular Medicine, The Herbert Wertheim UF Scripps Institute for Biomedical Innovation & Technology, Jupiter, Florida 33458, United States; pgriffin2@ufl.edu.

Supporting Information

The Supporting Information is available free of charge at https://pubs.acs.org/doi/10.1021/acs.analchem.3c00374.
Additional experimental methods and characterization results, including colorimetric standard curve, glycopeptide deglycosylation experiments, mass spectral data, peptide coverage maps from LC/MS–MS experiments, and deuterium uptake plots from HDX–MS (PDF)

Complete contact information is available at: https://pubs.acs.org/10.1021/acs.analchem.3c00374

The authors declare no competing financial interest.

Author Manuscript Author Manuscript Author Manuscript Author Manuscript

various buffer conditions and was employed in a column format that can be readily adapted into a typical HDX–MS platform. Using this system, we were able to obtain full sequence coverage of the SARS-CoV-2 receptor-binding domain (RBD) and map the glycosylated epitope of the glycan-binding mAb S309 to the RBD.

Graphical Abstract

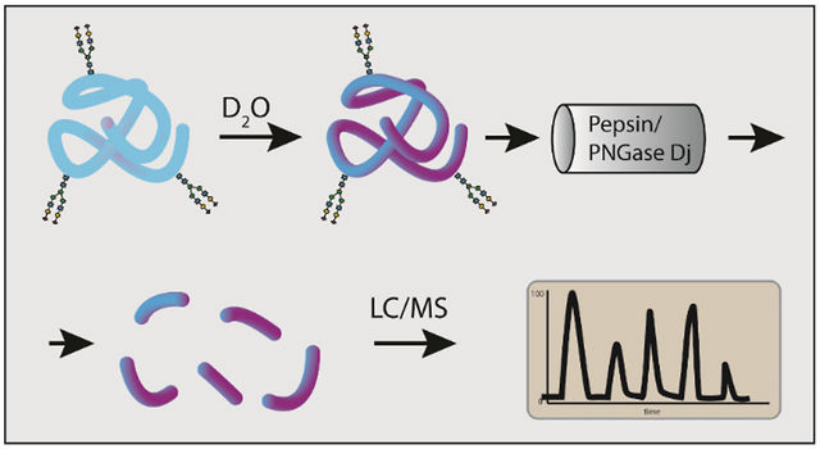

Hydrogen–deuterium exchange coupled with mass spectrometry (HDX–MS) is a method often used for antibody epitope mapping.[1–5] Recent examples include the use of HDX–MS to augment electron microscopy data for mapping the binding sites for a panel of monoclonal antibodies (mAbs) in the work that led to the discovery of LY-CoV555,[6] and for the screening of receptor-binding domain (RBD) epitopes in the development of the REGEN-COV mAb cocktail.[7] In a typical HDX–MS experiment, the protein of interest is incubated in a D_2O buffer, allowing the hydrogens to exchange with deuterium for set time periods. The samples are subsequently diluted with non-D_2O-containing buffers where the back-exchange of deuterated amides is slowed by reducing the temperature and maintaining the pH near 2.7, through the addition of a low-pH "quench" buffer.[8] While amide hydrogens in a random coil peptide at pH 7.0 and at room temperature exchange on a millisecond to second timescale, this may be reduced by a factor of up to 10^8 in a folded protein[8] Different features of protein structure can influence the rates of deuterium exchange, with contributions from factors including solvent accessibility and hydrogen bonding of the amide backbone.[8] To achieve spatial resolution, the protein is digested by proteases that are tolerant to low-pH slow-exchange conditions, and the resultant peptides are analyzed by liquid chromatography coupled with mass spectrometry (LC–MS). The extent of deuterium exchange at the peptide level is monitored with MS by comparing the shift in m/z of the isotopic envelope centroid to that of a control peptide not exposed to D_2O.[9]

Protein glycosylation can result in reduced peptide coverage in HDX–MS due to heterogeneous modification of peptides by glycans. To obtain a defined glycopeptide mass that can be monitored by MS, the structure of the glycan must first be resolved by specialized glycoproteomic methods prior to the HDX–MS experiment. Additionally, glycosylated amino acids are typically modified with multiple glycoforms at each site,[10]

Author Manuscript Author Manuscript Author Manuscript Author Manuscript

which can lead to diluted MS signals for glycopeptides. Glycan amide groups may also participate in exchange and potentially convolute deuterium uptake measurements.[11] The problem is pronounced, especially for viral spike proteins, which have evolved to evade immune detection through extensive modification with *N*-glycans.[12] In many HDX–MS studies involving SARS-CoV-2—especially when rapid results were critical—glycosylated positions were omitted from the analysis.[13–15] The SARS-CoV-2 RBD contains two *N*-glycans, at N331 and N343,[16] and several neutralizing mAbs targeting the RBD recognize epitopes containing the N343 glycan, including S309,[17] SW186,[18] SP1–77,[19] and C144,[20] which obscures their identification in HDX–MS.

Enzymatic removal of *N*-glycans following deuterium exchange has been a promising method to circumvent problems associated with glycosylation. A series of increasingly active and acid-tolerant enzymes have been recently uncovered and employed for HDX, from PNGase A[21,22] and PNGAse H^+[23] to the highly active PNGase Dj[24] and PNGase Rc.[25] These enzymes have typically been used in solutions for deglycosylation of glycopeptides; however, the Rand group employed PNGase Dj in an immobilized microfluidic enzyme reactor format through thiol–ene coupling to a monolithic matrix.[24] Here, we employ PNGase Dj for online deglycosylation in a standard format used for HDX protease columns, immobilized on aldehyde-modified polymeric resin and packed in an HPLC guard column that is straightforward to incorporate into a typical HDX platform. We applied this system to obtain full sequence coverage of the S protein RBD and to show extensive protection by the mAb S309, including at the site of the N343 glycan of the RBD.

EXPERIMENTAL SECTION

Glycopeptide Deglycosylation.

Glycopeptides were obtained by online digestion of α-1-acid glycoprotein (AGP) [25 μL of 110 μM AGP in phosphate-buffered saline (PBS) and 25 μL of 100 mM NaH_2PO_4 and 50 mM tris(2-carboxyethyl)phosphine hydrochloride (TCEP)] with a pepsin column [1 mm × 2 cm, 50 μL/min 0.1% trifluoroacetyl (TFA), 15 °C]. The resultant peptides/glycopeptides were desalted with a C18 column (Hypersil Gold, Thermo) using a linear gradient of 5–50% CH_3CN in 0.3% formic acid over 8 min. The eluted mixture of glycopeptides and peptides was dried and re-dissolved in PBS to give a solution corresponding to 2 μM AGP (or 0.2 μM for the reduced concentration to test the dynamic range). The glycopeptide/peptide mixture was diluted at a 1:1 ratio with 2× quench buffer (giving the final concentrations of quench buffer components listed in Figure 1) and injected onto a PNGase Dj column (1 mm × 2 cm, 50 μL/min 0.1% TFA) at an ambient temperature of 4 or 12 °C. The peptides were routed onto a C8 trap (Hypersil Gold, 1 × 10 mm, Thermo), followed by a C18 analytical column (Hypersil Gold, 1 × 50 mm, 3 μm particle size, Thermo) with a linear gradient of 4–40% CH_3CN in 0.3% formic acid over 8 min at a flow rate of 50 μL/min.[26,27] The peptides/glycopeptides were eluted into a mass spectrometer (Q Exactive, Thermo) with a resolution of 70,000. Injections were carried out in duplicate. Percent deglycosylation was calculated by comparing the intensity of the extracted ion chromatograms (EICs) (with 7 ppm error) for the target glycopeptide for samples analyzed with and without a PNGase Dj column. Representative mass spectra and EICs are shown in Figures S1 and S2.

Author Manuscript Author Manuscript Author Manuscript Author Manuscript

Peptide Identification.

Peptide maps of AGP, fetuin, horse radish peroxidase (HRP), and SARS-Cov-2 RBD were obtained with a Q Exactive mass spectrometer (Thermo) integrated with our HDX liquid chromatography platform.[28] The samples were mixed with a quench buffer and subjected to online protease/deglycosidase digestion (1 mm × 2 cm, 50 μL/min 0.1% TFA, 15 °C), then desalted (C8 trap column, Hypersil Gold, Thermo), and separated with a C18 analytical column (Hypersil Gold, Thermo; 70 min gradient of 4–40% CH_3CN in 0.3% formic acid). The tandem mass spectrometry (MS/MS) analysis consisted of top 10 ions with a dynamic exclusion of 30 s, an automated gain control of 1×10^5, and a maximum injection time of 80 ms. Data was analyzed with Mascot (version 2.8.1) with nonspecific cleavage, MS1 tolerance of 10 ppm, and MS2 fragment tolerance of 0.02 Da. Peptides with an ion score of 20 or more were included in the final peptide set, with select peptides having an ion score between 10 and 20 added after manual inspection and verification. Deamidation (at asparagine and glutamine) and oxidized methionine dynamic modifications were included in all searches.

HDX–MS Experiments.

HDX–MS experiments were carried out in a LEAP platform[28] kept at 4 °C and integrated with a high-resolution mass spectrometer, as described in earlier sections. For AGP, 10 μM samples in PBS were incubated for 1 h at 4 °C prior to the HDX–MS experiment. For SARS-CoV-2 RBD, the sample (10 μM in PBS) was equilibrated for 2 h at 4 °C, either as the apo-form, or with S309 (20 μM) or CR3022 (30 μM). After 1:5 dilution in D_2O buffer (20 mM NaH_2PO_4 and 150 mM NaCl, pH 7.6 at 4 °C) for various timepoints (0, 10, 60, 300, 900, and 3600 s), the samples were mixed with equal volumes of quench buffer (AGP: 0.1 mM NaH_2PO_4 and 50 mM TCEP; RBD: 3 M urea and 250 mM TCEP, pH 2.8), then digested/deglycosylated, desalted on a C8 trap column, separated on a C18 analytical column, and MS1 data was acquired (Q Exactive, Thermo, at 70,000 resolution). HDX analyses were performed in triplicate from a single preparation of an apo protein or a protein and a ligand. Data was analyzed with the software HDX workbench, with 100% deuterium incorporation calculated theoretically, and back-exchange-corrected using an assumed deuterium recovery rate of 70%.[27,29] Deamidated glycan sites were changed from asparagine to aspartic acid in the protein sequence.[30] All MS data has been submitted to the ProteomeXchange Consortium via the PRIDE[31] partner repository with the dataset identifier, PXD041204.

RESULTS AND DISCUSSION

Resin-Immobilized PNGase Dj Deglycosylated Glycopeptides under Various Buffer Conditions.

We expressed PNGase Dj in *Escherichia coli*[32] and immobilized it on POROS resin, a polymeric resin with a large surface area, that is routinely used by HDX labs for immobilization of pepsin and other proteases.[9,33,34] POROS 20 Al is an aldehyde-decorated resin that can be coupled to lysine side chains through Schiff base formation and subsequent reduction with cyanoborohydride.[34] Although porcine pepsin A is commonly immobilized on POROS resin, it only contains a single lysine and must be immobilized at pH 5.0,

Author Manuscript Author Manuscript Author Manuscript Author Manuscript

which is below the optimal pH for the coupling reaction.[35,36] We reasoned that PNGase Dj, which contains seven lysines and is stable at neutral pH[32] might couple to the resin more efficiently. Immobilization on resin was performed at pH 6.5, and the washed resin was packed into a micro-bore guard column.[36] PNGase Dj activity on the resin was determined with a colorimetric assay involving deglycosylation of HRP.[32] The immobilized PNGase Dj activity was assessed using a standard curve of in-solution PNGase Dj, and 1 mg of resin displayed an equivalent activity of 0.79 μg [95% CI: 0.66, 0.92] of solution-phase PNGase Dj (Figure S3).

The activity of immobilized PNGase Dj under common HDX–MS slow-exchange "quench" conditions was first assessed in column format by monitoring the deglycosylation of a glycopeptide, with column oven ambient temperatures of 12 and 4 °C (Figure 1). Protease columns employed in HDX–MS are often kept in column ovens maintained at a temperature range of 10–20 °C.[34,37–40] The immobilized enzyme appeared most susceptible to inhibition by guanidine HCl and showed resistance to the reducing agent TCEP (Figure 1A,C). To gauge the possible lasting effects of chaotropes or TCEP on column activity, we assessed deglycosylation immediately following injections containing high concentrations of chaotropes or TCEP (Figures 1C and S4). To control for dynamic range, several injections were performed at 1:10 dilution of glycopeptide (Figure S5). Additionally, we tested column activity in the presence of increasing TCEP concentrations by detecting deglycosylated bovine fetuin A glycopeptides EICs using the software HDX workbench with pepsin digestion followed by PNGase Dj (S6). For the three glycopeptides, increasing the TCEP concentration from 25 to 500 mM showed an average of 43% reduction in the peak area.

Peptide Mapping with PNGase Dj and Pepsin Improves the Sequence Coverage of Glycoproteins.

After confirming the activity of PNGase Dj, we assessed the column for deglycosylation of three glycoproteins: HRP, bovine fetuin A, and AGP. Prior to an HDX–MS experiment, a set of peptides that will be tracked in the HDX–MS experiment must first be identified with MS/MS. As glycopeptides are deglycosylated faster than intact proteins, we employed a dual column setup, with proteins moving first through the pepsin column and then into the deglycosidase column. To simplify the setup, we also used a mixed-bed column with a single column containing a 9:1 mixture of pepsin and PNGase Dj resin. A mixed-bed column with pepsin and PNGase Dj may also enhance proteolysis, with deglycosylation allowing pepsin further access to cleavage sites. We observed coverage at *N*-glycan sites (Figures 2, S7, and S8), while these sites lacked coverage when digested with pepsin alone. Samples treated with PNGase Dj showed deamidation at *N*-glycan asparagines, while no deamidated peptides were detected with pepsin alone. In all cases, the inclusion of PNGase Dj gave improved coverage, and the mixed-bed results were comparable to those of the dualcolumn. The mixed-bed system also showed peptides with termini closer to the *N*-glycan site, indicating that deglycosylation may have allowed pepsin further cleavage near glycan sites.

Author Manuscript Author Manuscript Author Manuscript Author Manuscript

Removal of AGP *N*-Glycans Prior to HDX–MS Alters Its Deuterium Uptake Profile.

Initial HDX–MS studies focused on AGP, a highly glycosylated plasma protein. The glycan structure of AGP is known to affect its numerous drug-binding interactions.[41,42] We evaluated the effects of glycosylation on the dynamics of AGP by treating it with PNGase F (a deglycosidase that functions in neutral pH conditions) prior to the HDX–MS experiment. Both native and PNGase F-treated AGP were digested with the mixed-bed column following HDX. The results showed substantial perturbation of AGP by PNGase F treatment (Figures S9–S11). Glycosylation at N38 appears to provide protection from exchange (with PNGase F-treated AGP showing increased D uptake vs native), and protection was observed in several sheets and helices clustered around N38. At the loop proximal to the N54 glycan site, PNGase F-treated AGP showed further perturbation, in this case by way of exhibiting moderate deprotection.

Online Immobilized PNGase Dj Allows HDX–MS Mapping of S309 Glycosylated Epitope on the SARS-CoV-2 RBD.

Next, we used HDX–MS to analyze the interaction of the SARS-CoV-2 RBD sequence with mAbs. S309 is an antibody isolated from B cells of a patient previously infected with SARS-CoV-1 and is cross-reactive with SARS-CoV-2. The interaction between S309 and the S trimer was characterized by cryogenic electron microscopy (cryo-EM), and S309 was shown to recognize an epitope on the RBD near the N343 glycan, including contact with the glycan itself.[17] We digested an RBD-Fc fusion protein with a mixed-bed pepsin/PNGase Dj column and compared its digestion with a pepsin column. While the mixed-bed column afforded full coverage of the RBD, pepsin lacked coverage in the region of N331 and N343 glycans (Figures S12 and S13).

With full coverage of the RBD sequence, we moved to a differential HDX–MS experiment, evaluating deuterium uptake on the RBD in the presence and absence of S309. HDX–MS results revealed that deglycosylated peptides were detected at all *N*-glycan sites on the sequence, and both positions, N343 and N630, showed multiple overlapping deglycosylated peptides (Figures S14–S16). The greatest magnitude of protection was centered around the N343 glycan, from residues 338 to 350 (Figures 3 and S14). This extended into a beta sheet in the core of the RBD, from 350 to 364. Protection was also seen on residues 434–441 on the boundary of the ACE2 receptor-binding motif (RBM, consisting of residues 438–506). The RBD was present as an Fc fusion protein, but no significant differential HDX was observed in the Fc tag. These results aligned well with the epitope identified through cryo-EM. The authors of that work identified RBD residues 337–344, 356–361, and 440–444 as the S309 epitope.[17] We also observed protection in residues 516–533 near the C-terminus of the RBD. Although this sequence does not directly interact with S309, residues 521– 527 make extensive contact with 358–364, which may have induced an allosteric change upon S309 binding.

Epitope Mapping of the mAb CR3022 to a Nonglycosylated Region of SARS-CoV-2 RBD.

Finally, differential HDX was performed with a different mAb with an epitope outside the glycosylated region of the RBD. Like S309, CR3022 is also cross-reactive with both SARS-CoV-1 and SARS-CoV-2. It recognizes a glycosylated epitope on the SARS-CoV-1 RBD,

Author Manuscript Author Manuscript Author Manuscript Author Manuscript

but the analogous sequence in the SARS-CoV-2 RBD lacks glycosylation.[43] We observed protection in the beta sheet in residues 376–387 and 423–43, which matched closely with the results reported by the crystal structure of CR3022 and the SARS-CoV-2 RBD (Figures S17–S20). We did not see protection in the glycosylated region near the RBD N-terminal.

CONCLUSIONS

Immobilization of PNGase Dj on POROS resin provides a straightforward means of increasing sequence coverage for HDX–MS analysis of glycoproteins, allowing deglycosylation following hydrogen–deuterium exchange. The methods for immobilization employed here may be suitable for other PNGase enzymes, such as PNGase Rc. PNGase Rc is a recently discovered glycosidase with exceptionally high activity in low-pH conditions[44] and has been used for in-solution deglycosylation of peptides for HDX–MS.[25] It is homologous to PNGase Dj with 45% sequence identification, and the recombinant protein is reported to have been obtained in good yields.[25] In general, glycans may influence protein-binding events as well as altering conformations distal to the glycosylation site, making it desirable to perform HDX on native proteins, rather than those that have been enzymatically deglycosylated prior to the HDX experiment or expressed in *E. coli*.[21,45] Indeed, the results shown here with AGP indicate that glycosylation has an impact on protein conformation, with glycans appearing to stabilize some regions, while increasing the dynamics in other areas of the protein.

The immobilized, column-format PNGase Dj allowed coverage of the glycosylated RBD epitope for S309, with results in close agreement with the cryo-EM structure.[17] RBD mutations N440K and G339D in SARS-CoV-2 omicron variants greatly reduced the effectiveness of S309,[46] also in agreement with our data. We also mapped the epitope of CR3022 to a distal site on the RBD, which showed no protection on glycosylated peptides, indicating the PNGase Dj treatment did not introduce artifacts. HDX–MS is a rapid method for mapping antibody-binding sites, and here, we show the results that augment data from cryo-EM and crystallography studies. In addition to being generally applicable to glycoproteins, this method could be especially valuable for other highly glycosylated viral spike proteins, such as those of HIV, where potent neutralizing antibodies have also been shown to recognize glycosylated epitopes.[47,48]

Supplementary Material

Refer to Web version on PubMed Central for supplementary material.

ACKNOWLEDGMENTS

Molecular graphics were produced with Pymol (The PyMOL Molecular Graphics System, Schrödinger, LLC) and Maestro (Maestro, Schrödinger, LLC, New York, NY, 2021). This work was funded by the Behavior of HIV in Viral Environments (B-HIVE) Center of the NIH with the grant U54 AI170855.

REFERENCES

(1). Francino-Urdaniz IM; Whitehead TA RSC Chem. Biol 2021, 2, 1580–1589. [PubMed: 34977572]

Author Manuscript Author Manuscript Author Manuscript Author Manuscript

(2). Grauslund LR; Calvaresi V; Pansegrau W; Norais N; Rand KD J. Am. Soc. Mass Spectrom 2021, 32, 1575–1582. [PubMed: 33683906]

(3). Gramlich M; Hays HCW; Crichton S; Kaiser PD; Heine A; Schneiderhan-Marra N; Rothbauer U; Stoll D; Maier S; Zeck A Antibodies 2021, 10, 11. [PubMed: 33808657]

(4). Brown KA; Lento C; Rajendran S; Dowd J; Wilson DJ Biochemistry 2020, 59, 2776–2781. [PubMed: 32672953]

(5). Bereszczak JZ; Rose RJ; van Duijn E; Watts NR; Wingfield PT; Steven AC; Heck AJR J. Am. Chem. Soc 2013, 135, 6504–6512. [PubMed: 23597076]

(6). Jones BE; Brown-Augsburger PL; Corbett KS; Westendorf K; Davies J; Cujec TP; Wiethoff CM; Blackbourne JL; Heinz BA; Foster D; et al. Sci. Transl. Med 2021, 13, No. eabf1906.

(7). Hansen J; Baum A; Pascal KE; Russo V; Giordano S; Wloga E; Fulton BO; Yan Y; Koon K; Patel K; et al. Science 2020, 369, 1010–1014. [PubMed: 32540901]

(8). Chalmers MJ; Busby SA; Pascal BD; West GM; Griffin PR Expert Rev. Proteomics 2011, 8, 43–59. [PubMed: 21329427]

(9). Hamuro Y; Coales SJ J. Am. Soc. Mass Spectrom 2018, 29, 623–629. [PubMed: 29299838]

(10). An HJ; Froehlich JW; Lebrilla CB Curr. Opin. Chem. Biol 2009, 13, 421–426. [PubMed: 19700364]

(11). Guttman M; Scian M; Lee KK Anal. Chem 2011, 83, 7492–7499. [PubMed: 21863800]

(12). Watanabe Y; Bowden TA; Wilson IA; Crispin M Biochim. Biophys. Acta, Gen. Subj 2019, 1863, 1480–1497. [PubMed: 31121217]

(13). Raghuvamsi PV; Tulsian NK; Samsudin F; Qian X; Purushotorman K; Yue G; Kozma MM; Hwa WY; Lescar J; Bond PJ; et al. eLife 2021, 10, No. e63646.

(14). Seow J; Khan H; Rosa A; Calvaresi V; Graham C; Pickering S; Pye VE; Cronin NB; Huettner I; Malim MH; et al. Cell Rep. 2022, 40, 111276. [PubMed: 35981534]

(15). Narang D; James DA; Balmer MT; Wilson DJ J. Am. Soc. Mass Spectrom 2021, 32, 1593–1600. [PubMed: 33794092]

(16). Watanabe Y; Allen JD; Wrapp D; McLellan JS; Crispin M Science 2020, 369, 330–333. [PubMed: 32366695]

(17). Pinto D; Park Y-J; Beltramello M; Walls AC; Tortorici MA; Bianchi S; Jaconi S; Culap K; Zatta F; De Marco A; et al. Nature 2020, 583, 290–295. [PubMed: 32422645]

(18). Fang Y; Sun P; Xie X; Du M; Du F; Ye J; Kalveram BK; Plante JA; Plante KS; Li B; et al. Sci. Immunol 2022, 7, No. eabp9962.

(19). Luo S; Zhang J; Kreutzberger AJB; Eaton A; Edwards RJ; Jing C; Dai H-Q; Sempowski GD; Cronin K; Parks R; et al. Sci. Immunol 2022, 7, No. eadd5446.

(20). Barnes CO; Jette CA; Abernathy ME; Dam KMA; Esswein SR; Gristick HB; Malyutin AG; Sharaf NG; Huey-Tubman KE; Lee YE; et al. Nature 2020, 588, 682–687. [PubMed: 33045718]

(21). Wagner ND; Huang Y; Liu T; Gross ML J. Am. Soc. Mass Spectrom 2021, 32, 1638–1643. [PubMed: 33625217]

(22). Jensen PF; Comamala G; Trelle MB; Madsen JB; Jørgensen TJ; Rand KD Anal. Chem 2016, 88, 12479–12488. [PubMed: 28193043]

(23). Comamala G; Madsen JB; Voglmeir J; Du YM; Jensen PF; Østerlund EC; Trelle MB; Jørgensen TJD; Rand KD J. Am. Soc. Mass Spectrom 2020, 31, 2305–2312. [PubMed: 32955262]

(24). Comamala G; Krogh CC; Nielsen VS; Kutter JP; Voglmeir J; Rand KD Anal. Chem 2021, 93, 16330–16340. [PubMed: 34843209]

(25). Gramlich M; Maier S; Kaiser PD; Traenkle B; Wagner TR; Voglmeir J; Stoll D; Rothbauer U; Zeck A Anal. Chem 2022, 94, 9863–9871. [PubMed: 35749695]

(26). Zheng J; Chang MR; Stites RE; Wang Y; Bruning JB; Pascal BD; Novick SJ; Garcia-Ordonez RD; Stayrook KR; Chalmers MJ; et al. Nat. Commun 2017, 8, 923. [PubMed: 29030554]

(27). Tuske S; Zheng J; Olson ED; Ruiz FX; Pascal BD; Hoang A; Bauman JD; Das K; DeStefano JJ; Musier-Forsyth K; et al. Curr. Res. Struct. Biol 2020, 2, 116–129. [PubMed: 33870216]

(28). Chalmers MJ; Busby SA; Pascal BD; He Y; Hendrickson CL; Marshall AG; Griffin PR Anal. Chem 2006, 78, 1005–1014. [PubMed: 16478090]

Author Manuscript Author Manuscript Author Manuscript Author Manuscript

(29). Zheng J; Corzo C; Chang MR; Shang J; Lam VQ; Brust R; Blayo A-L; Bruning JB; Kamenecka TM; Kojetin DJ; et al. Structure 2018, 26, 1431–1439.e6. [PubMed: 30146169]

(30). Pascal BD; Willis S; Lauer JL; Landgraf RR; West GM; Marciano D; Novick S; Goswami D; Chalmers MJ; Griffin PR J. Am. Soc. Mass Spectrom 2012, 23, 1512–1521. [PubMed: 22692830]

(31). Perez-Riverol Y; Csordas A; Bai J; Bernal-Llinares M; Hewapathirana S; Kundu DJ; Inuganti A; Griss J; Mayer G; Eisenacher M; et al. Nucleic Acids Res. 2019, 47, D442–d450. [PubMed: 30395289]

(32). Guo RR; Comamala G; Yang HH; Gramlich M; Du YM; Wang T; Zeck A; Rand KD; Liu L; Voglmeir J Front. Bioeng. Biotechnol 2020, 8, 741. [PubMed: 32719787]

(33). Ahn J; Jung MC; Wyndham K; Yu YQ; Engen JR Anal. Chem 2012, 84, 7256–7262. [PubMed: 22856522]

(34). Zheng J; Strutzenberg TS; Reich A; Dharmarajan V; Pascal BD; Crynen GC; Novick SJ; Garcia-Ordonez RD; Griffin PR Anal. Chem 2020, 92, 11018–11028. [PubMed: 32658454]

(35). Morellon-Sterling R; Tavano O; Bolivar JM; Berenguer-Murcia Á; Vela-Gutiérrez G; Sabir JSM; Tacias-Pascacio VG; Fernandez-Lafuente R Int. J. Biol. Macromol 2022, 210, 682–702. [PubMed: 35508226]

(36). Busby SA; Chalmers MJ; Griffin PR Int. J. Mass Spectrom 2007, 259, 130–139.

(37). Eisinger ML; Dörrbaum AR; Michel H; Padan E; Langer JD Proc. Natl. Acad. Sci. U.S.A 2017, 114, 11691–11696. [PubMed: 29078272]

(38). Javed W; Vallet S; Clement M-P; Le Roy A; Moulin M; Härtlein M; Breyton C; Burlet-Schiltz O; Marcoux J; Orelle C; et al. J. Mol. Biol 2022, 434, 167541. [PubMed: 35292347]

(39). Wales TE; Fadgen KE; Gerhardt GC; Engen JR Anal. Chem 2008, 80, 6815–6820. [PubMed: 18672890]

(40). Domnowski M; Lo Presti K; Binder J; Reindl J; Lehmann L; Kummer F; Wolber M; Satzger M; Dehling M; Jaehrling J; et al. Mol. Pharm 2021, 18, 236–245. [PubMed: 33331157]

(41). Wu D; Struwe WB; Harvey DJ; Ferguson MAJ; Robinson CV Proc. Natl. Acad. Sci. U.S.A 2018, 115, 8763–8768. [PubMed: 30111543]

(42). Huang RYC; Hudgens JW Biochemistry 2013, 52, 7127–7136. [PubMed: 24041412]

(43). Yuan M; Wu NC; Zhu X; Lee CD; So RTY; Lv H; Mok CKP; Wilson IA Science 2020, 368, 630–633. [PubMed: 32245784]

(44). Guo RR; Zhang TC; Lambert TOT; Wang T; Voglmeir J; Rand KD; Liu L Rapid Commun. Mass Spectrom 2022, 36, No. e9376.

(45). Anderson KW; Bergonzo C; Scott K; Karageorgos IL; Gallagher ES; Tayi VS; Butler M; Hudgens JW J. Mol. Biol 2022, 434, 167391. [PubMed: 34890647]

(46). VanBlargan LA; Errico JM; Halfmann PJ; Zost SJ; Crowe JE Jr.; Purcell LA; Kawaoka Y; Corti D; Fremont DH; Diamond MS Nat. Med 2022, 28, 490–495. [PubMed: 35046573]

(47). Willis JR; Berndsen ZT; Ma KM; Steichen JM; Schiffner T; Landais E; Liguori A; Kalyuzhniy O; Allen JD; Baboo S; et al. Immunity 2022, 55, 2149–2167.e9. [PubMed: 36179689]

(48). Garces F; Sok D; Kong L; McBride R; Kim HJ; Saye-Francisco KF; Julien JP; Hua Y; Cupo A; Moore JP; et al. Cell 2014, 159, 69–79. [PubMed: 25259921]

Author Manuscript Author Manuscript Author Manuscript Author Manuscript

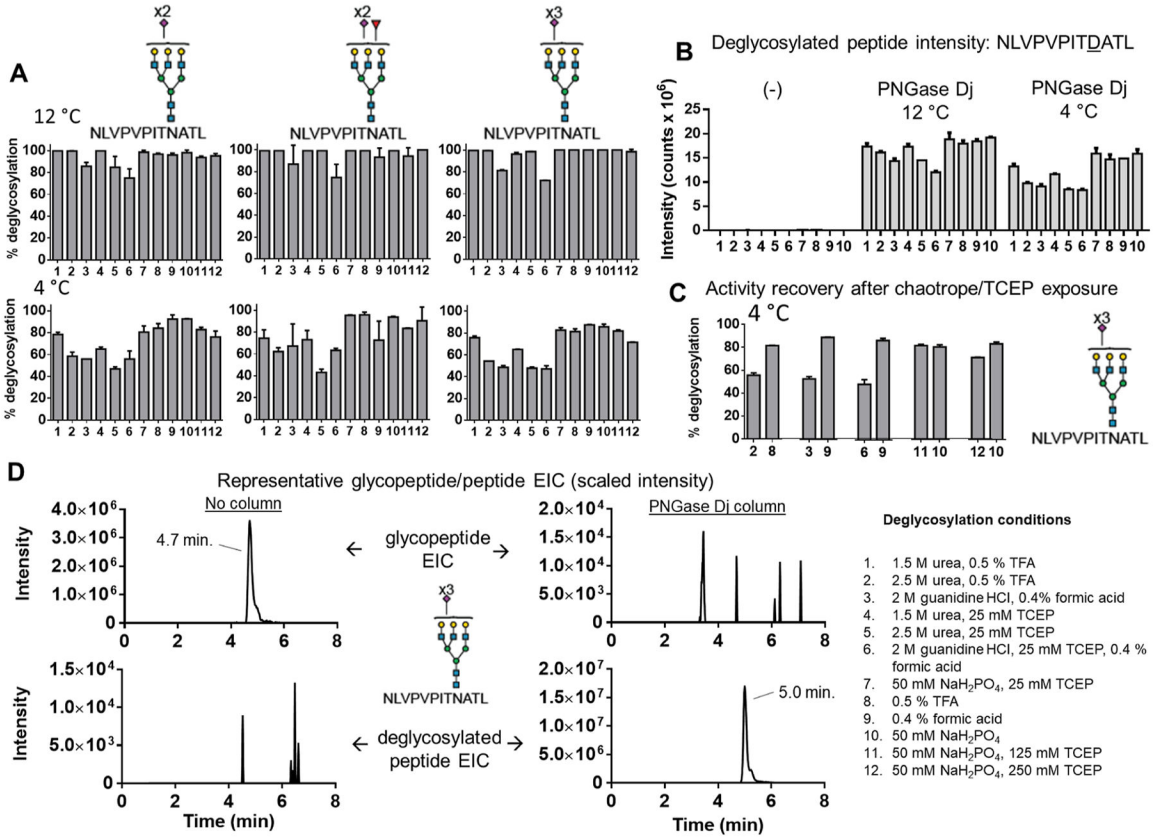

Figure 1.

Deglycosylation of glycopeptide by immobilized PNGase Dj. (A) Deglycosylation of glycopeptides in various buffers. The numbers on the *x* axis correspond to the list of deglycosylation conditions. (B) Signals for deglycosylated peptides are greatly enhanced in PNGase Dj-treated samples. (C) Each pair of bars in the plot show chaotrope/TCEP injection followed by the respective reference buffer injection. (D) Representative EICs for glycopeptide in 50 mM NaH_2PO_4 and 25 mM TCEP at 12 °C. The intensity is scaled to each plot.

Author Manuscript Author Manuscript Author Manuscript Author Manuscript

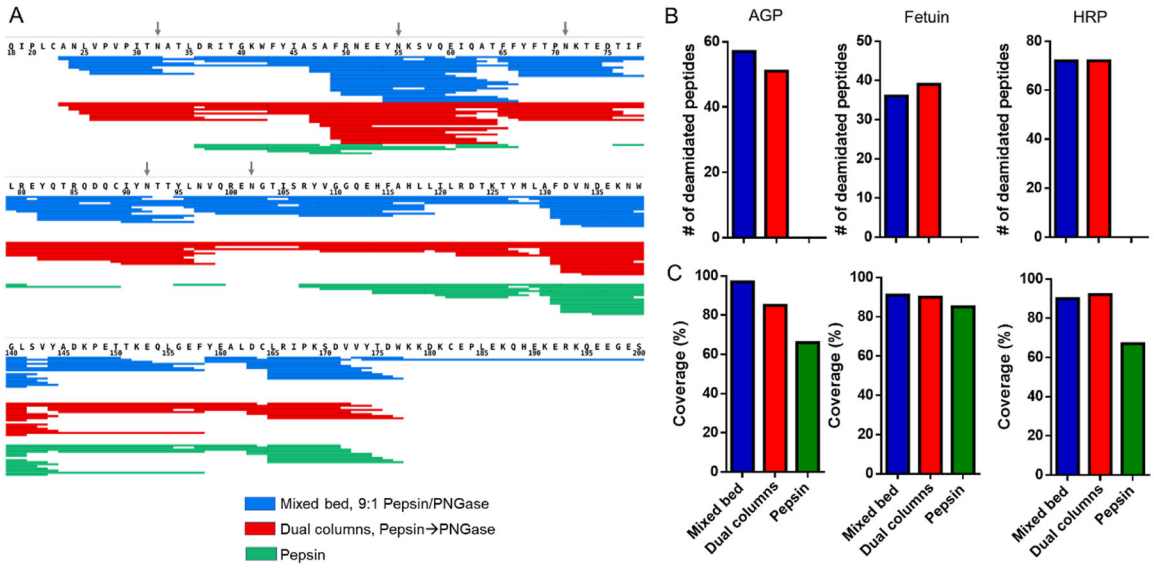

Figure 2.

LC–MS/MS peptide coverage of glycoproteins AGP, fetuin A, and HRP. (A) Peptide coverage map of AGP. *N*-Glycan sites are marked with an arrow. (B) Number of deamidated peptides detected. (C) Percent coverage of each glycoprotein sequence.

Author Manuscript Author Manuscript Author Manuscript Author Manuscript

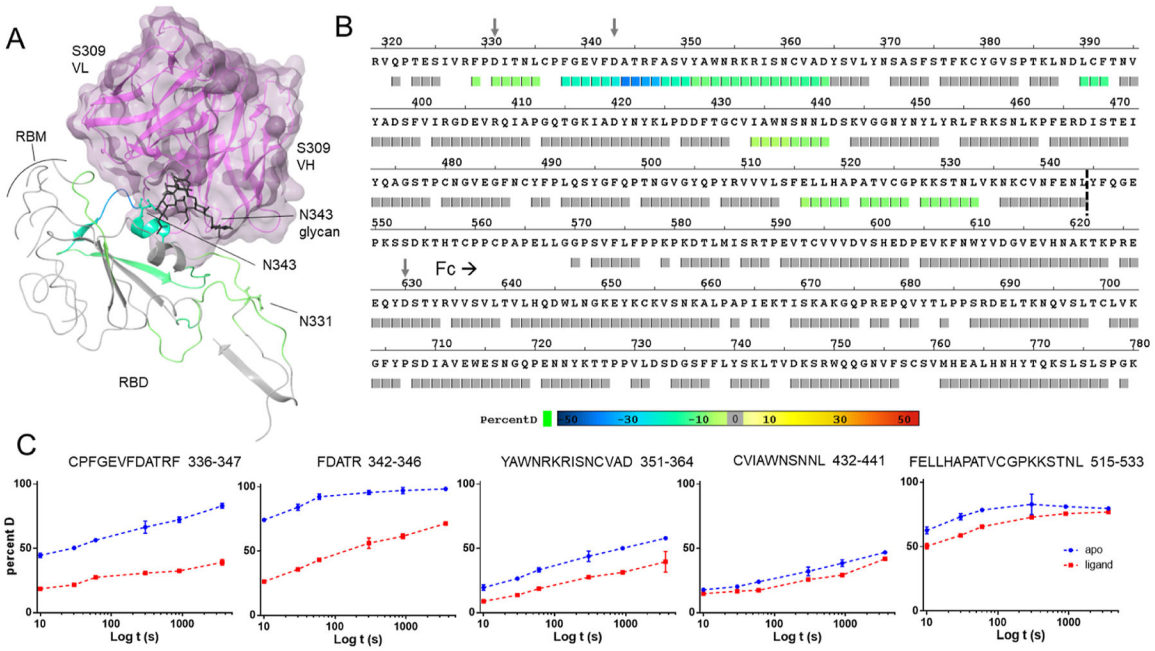

Figure 3.

S309 interaction with glycosylated RBD epitope probed by HDX. (A) Deuterium uptake differential mapped to the RBD region of the cryo-EM structure of S309 and the S protein trimer (PDB file 6WPS). (B) Consolidated difference plot with the RBD-Fc fusion protein sequence. N-Glycosylated sites are shown with arrows and are deamidated to aspartic acid due to deglycosylation. (C) Representative buildup curves across regions showing protection.